

Similarity transformation for equilibrium boundary layers, including effects of blowing and suction

Xi Chen* and Fazle Hussain

Department of Mechanical Engineering, Texas Tech University, Lubbock, Texas 79409-1021, USA

(Received 2 December 2016; published 27 March 2017)

We present a similarity transformation for the mean velocity profiles in sink flow turbulent boundary layers, including effects of blowing and suction. It is based on symmetry analysis which transforms the governing partial differential equations (for mean mass and momentum) into an ordinary differential equation and yields a new result including an exact, linear relation between the mean normal (V) and streamwise (U) velocities. A characteristic length function is further introduced which, under a first order expansion (whose coefficient is η) in wall blowing and suction velocity, leads to the similarity transformation for U with the value of $\eta \approx -1/9$. This transformation is shown to be a group invariant and maps different U profiles under different blowing and suction conditions into a (universal) profile for no blowing or suction. Its inverse transformation enables predictions of all mean quantities in the mean mass and momentum equations, in good agreement with DNS data.

DOI: [10.1103/PhysRevFluids.2.034605](https://doi.org/10.1103/PhysRevFluids.2.034605)

I. INTRODUCTION

Equilibrium, denoted by the self-similarity (or self-preservation) of the mean profiles under proper normalization [1], is one of the most fundamental concepts in turbulent boundary layers (TBLs). It is classified into two broad categories [2]. One case involves an approximate equilibrium where the velocity and Reynolds stresses are self-similar over most of the boundary layer, and the other is an exact equilibrium where the self-similarity is observed over the entire layer thickness. The zero-pressure-gradient (ZPG) TBL, containing two independent (inner and outer) scales with the similarity properties expressed as the “law of the wall” and “defect law” [3], belongs to the first category. In contrast, the sink-flow boundary layer, a counterpart of the laminar Falkner-Skan boundary layers and a generic Jeffery-Hamel flow constrained by two smooth plane surfaces, possesses many interesting properties [4,5]. This flow has an invariant velocity profile, a zero mean entrainment, radial mean streamlines, a constant Reynolds number (Re), and a constant friction coefficient along the stream, rendering it as the purest example of an exact equilibrium TBL [6], and has triggered numerous studies on the scaling and flow structures [4,7–9].

Whereas the laminar sink flow is one of the few known exact solutions of the Navier-Stokes equations [10], there is no known solution for the turbulent sink flow due to the Reynolds shear stress. This is analogous to the ZPG TBL, where various models are developed for the unclosed mean momentum equation. Notable works include an asymptotic logarithmic law for the mean velocity [4,5,11], the mixing length hypothesis [12], etc. However, to emphasize, except for the logarithmic law, few are known for the sink flow TBLs. A crucial question concerns how the exact equilibrium state is produced [6] and whether the state is robust under various boundary conditions. This is important because so far only the sink-flow TBL is known to display the exact equilibrium state (first shown by Townsend [13] and Rotta [14]). To pursue more possible self-similarities in wall flows, a general theoretical framework is thus needed which is developed in this paper.

Here, we use the Lie group symmetry analysis [10,15] to derive the self-similarity equation for boundary layers including effects of blowing and suction. It follows a recent work by She *et al.* [16] with a notable difference, viz., it transforms the mean mass and mean momentum equations to a

*xi.chen@ttu.edu

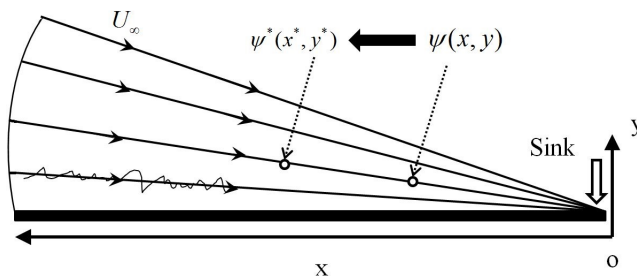


FIG. 1. Sketch of a sink-flow turbulent boundary layer and the symmetry transformation from $\psi(x, y)$ to $\psi^*(x^*, y^*)$ following (9), i.e., from location (x, y) to (x^*, y^*) .

streamwise independent ordinary differential equation (ODE) and presents the necessary boundary conditions for the existence of the exact equilibrium state. It systematically unifies the Falkner-Skan laminar flows and the sink-flow TBLs having different pressure gradients and blowing and suction, thus covering a wide class of equilibrium flows and perhaps fostering a more general study in the future. The approach is more general than previous scaling analysis [1,5] where specific scales are proposed for specific flows. Also note that while only the laminar cases (Blasius and Falkner-Skan) have been studied through a symmetry analysis by Cantwell [10], as well as the smooth wall turbulent boundary layers by Oberlack [17], we extend the symmetry analysis to include the Reynolds shear stress and blowing and suction.

More importantly, we establish a similarity transformation for the mean velocity profile covering ranges of blowing and suction strengths. This transformation is found to be a group invariant (in most of the flow region except the buffer layer) and maps different U profiles under different blowing and suction conditions into a universal profile under no blowing or suction. The latter reversely enables calculations of all quantities in the mean mass and momentum equations—in good agreement with direct numerical simulation (DNS) data [18]. The results indicate that the wall blowing and suction not only preserve the equilibrium condition but also lead to a new similarity among different blowing and suction strengths.

The paper is thus organized as follows. Section II is devoted to a symmetry analysis of the mean mass and streamwise mean momentum equations, resulting a generalized ODE for various flows mentioned above. The similarity transformation for U is presented in Sec. III; also included is a prediction of the mean velocities. Section IV presents the conclusions and discussions.

II. SYMMETRY TRANSFORMATION FOR THE BOUNDARY LAYER EQUATIONS

The incompressible, two-dimensional Navier-Stokes equations with the standard boundary layer approximation (NSBL) read

$$\frac{\partial U}{\partial x} + \frac{\partial V}{\partial y} = 0, \quad (1)$$

$$U \frac{\partial U}{\partial x} + V \frac{\partial U}{\partial y} = U_\infty \frac{\partial U_\infty}{\partial x} + \nu \frac{\partial^2 U}{\partial y^2} - \frac{\partial R}{\partial y}, \quad (2)$$

where U and V indicate mean streamwise (x) and wall normal y velocities; $R = \langle u'v' \rangle$ is the Reynolds shear stress. Note that a zero R indicates the laminar flow. The boundary conditions are $U(y=0) = 0$, $U(y \rightarrow \infty) = U_\infty(x)$, and $V(y=0) = V_w(x)$, where a zero V_w indicates the nonpenetrating wall and else for suction (a negative V_w) and blowing (a positive V_w) effects. Note that the origin location $(x, y) = (0, 0)$ is set at the sink apex shown in Fig. 1, to explain the dilation transformation defined later.

Similar to the analysis of the laminar boundary layer flow, we introduce the stream function to eliminate the mass equation. The novelty is that, due to blowing and suction effects, the velocities are

$$U = \psi_y, \quad V = -\psi_x + V_w. \quad (3)$$

One can check that (3) always satisfies (1) as long as $\psi_{xy} = \psi_{yx}$, common to previous analysis [10]. Therefore, (2) written in stream function reads

$$\psi_y \psi_{xy} - \psi_x \psi_{yy} + V_w \psi_{yy} = U_\infty \partial_x U_\infty + \nu \psi_{yyy} - R_y, \quad (4)$$

where $V_w \psi_{yy}$ and $R_y = \partial_y R$ are additional compared to the Falkner-Skan equation. The idea of symmetry analysis is that, once a specific solution (U_∞, V_w, ψ, R) at the position (x, y) is given, a series of solutions can be obtained under the group transformations. These transformations can be calculated by requiring that the transformed variables $(x^*, y^*, U_\infty^*, V_w^*, \psi^*, R^*)$ satisfy the same governing equation (4), also satisfied by untransformed variables (U_∞, V_w, ψ, R) . Technically, such transformations can be obtained via mathematical software such as MAPLE, and the resultant group invariants (easily obtained by eliminating group parameters) can be used as similarity variables to readily transform the partial differential equation (PDE) to an ODE. This is different from the sophisticated dimensional analysis where the similarity variables are mostly obtained by trial and error [10]. Here, following the customary procedure, we search for the dilation symmetry permitted by (4) and show how (4) is transformed to an ODE; for more symmetries permitted by (4) in terms of infinitesimals, see the Appendix.

Denote the dilations as

$$\begin{aligned} x^* &= e^{a_1} x, & y^* &= e^{a_2} y, & U_\infty^* &= e^{a_3} U_\infty, \\ V_w^* &= e^{a_4} V_w, & \psi^* &= e^{a_5} \psi, & R^* &= e^{a_6} R, \end{aligned} \quad (5)$$

where $a_6 = a_3 + a_4$, as made apparent in (7) and (8) later. This indicates that the dilation for R depends on the dilations for the velocities since R is a product of u' and v' . Substituting (5) into (4), we obtain

$$\begin{aligned} &e^{(2a_2+a_1-2a_5)} \psi_{y^*}^* \psi_{x^* y^*}^* - e^{(2a_2+a_1-2a_5)} \psi_{x^*}^* \psi_{y^* y^*}^* + e^{(2a_2-a_4-a_5)} V_w^* \psi_{y^* y^*}^* \\ &= e^{(a_1-2a_3)} U_\infty^* \partial_{x^*} U_\infty^* + e^{(3a_2-a_5)} \nu \psi_{y^* y^* y^*}^* - e^{(a_2-a_6)} R_{y^*}^*. \end{aligned} \quad (6)$$

The dilation symmetry of (4) requires

$$2a_2 + a_1 - 2a_5 = 2a_2 - a_4 - a_5 = a_1 - 2a_3 = 3a_2 - a_5 = a_2 - a_6, \quad (7)$$

where four of the six free coefficients a_i ($i = 1, 2, \dots, 6$) can be determined from (7). Without losing generality, we denote the two free coefficients as $a_1 = \varepsilon$ and $a_3 = \beta\varepsilon$. Thus, the other four are given as

$$\begin{aligned} a_2 &= (1 - \beta)\varepsilon/2, & a_4 &= (\beta - 1)\varepsilon/2, \\ a_5 &= (1 + \beta)\varepsilon/2, & a_6 &= (3\beta - 1)\varepsilon/2. \end{aligned} \quad (8)$$

Substituting (8) back into (5) yields the two-parameter $(\varepsilon, \beta \in \mathbf{R})$ dilation symmetry group:

$$\begin{aligned} x^* &= e^\varepsilon x, & y^* &= e^{(1-\beta)\varepsilon/2} y, & U_\infty^* &= e^{\beta\varepsilon} U_\infty, \\ V_w^* &= e^{(\beta-1)\varepsilon/2} V_w, & \psi^* &= e^{(1+\beta)\varepsilon/2} \psi, & R^* &= e^{(3\beta-1)\varepsilon/2} R, \end{aligned} \quad (9)$$

which has a clear explanation, i.e., a mapping of a solution at the location (x, y) to a series of solutions at locations (x^*, y^*) in the sink flow when the two parameters ε and β vary (see Fig. 1). Note that translations for x , y , ψ , and R also keep (4) invariant, which, however, break the invariance of wall conditions $\psi(x=0) = 0$ and $R(y=0) = 0$, and hence are not considered here.

An important fact is that the symmetry group (9) implies the necessary boundary conditions for the existence of the equilibrium state (i.e., the similarity solution) as follows. By integrating the characteristic equations of (9), i.e.,

$$\begin{aligned} \frac{dx}{x} &= \frac{dy}{(1-\beta)y/2} = \frac{dU_\infty}{\beta U_\infty} = \frac{dV_w}{(\beta-1)V_w/2} \\ &= \frac{d\psi}{(1+\beta)\psi/2} = \frac{dR}{(3\beta-1)R/2}, \end{aligned} \quad (10)$$

we obtain five independent dilation invariants:

$$\begin{aligned} I_1 &= y/x^{(1-\beta)/2}, \quad I_2 = U_\infty/x^\beta, \quad I_3 = V_w/x^{(\beta-1)/2}, \\ I_4 &= \psi/x^{(1+\beta)/2}, \quad I_5 = R/x^{(3\beta-1)/2}, \end{aligned} \quad (11)$$

which are explained in order. The first invariant I_1 , in analogy to the similarity variable $\chi = y/\sqrt{\nu x/U_\infty}$ in the Blasius equation, describes the characteristic line of the dilation, i.e., $y = I_1 x^{(1-\beta)/2}$. The second invariant I_2 indicates that the pressure gradient parameter $K_p \equiv \nu \partial_x U_\infty / U_\infty^2$, widely used in the literature (e.g., [5,6]), must satisfy

$$K_p = \nu \beta / (I_2 x^{\beta+1}) \propto x^{-1-\beta}, \quad (12)$$

where $U_\infty = I_2 x^\beta$ is substituted. Moreover, I_3 requires a streamwise dependent blowing and suction velocity $V_w \propto x^{(1-\beta)/2}$. Finally, I_4 and I_5 respectively indicate the invariants along the characteristic lines, composed of ψ and R (both are dependent variables) with x .

Here, we are particularly interested in the specific case $\beta = -1$, which corresponds to the sink-flow TBL. It is known that for sink TBL, the boundary conditions are $U_\infty \propto 1/x$ and $K_p = \text{const}$ [5,6]. Then, (12) yields $\beta = -1$. In fact, taking $\beta = -1$, we have $y = I_1 x$ corresponding to the radial mean streamline in Fig. 1 [5]. Moreover, $I_2 = U_\infty x$ indicates the sink strength in [4], and $V_w \propto U_\infty \propto 1/x$ is the exact blowing and suction setting in the DNS by Patwardhan [18]. In such a case, ψ is invariant under dilation as sketched in Fig. 1. Note that all of the group parameters are independent of viscosity (or Re). Such a Re-independent dilation invariance should be considered a significant property of the sink-flow TBL, because the symmetry could be physically identified in the flow field without changing the viscosity (by different fluids).

Furthermore, the PDE system (1) and (2) is now transformed to an ODE under (9). Before we proceed, it is natural to normalize the above invariants to be dimensionless using ν (viscosity) and I_2 (sink strength) [10], which are

$$\begin{aligned} \alpha &= I_1 \sqrt{-I_2/\nu} = y \sqrt{-U_\infty/(x\nu)}, \\ \gamma &= I_3 / \sqrt{-I_2\nu} = V_w / \sqrt{-U_\infty\nu/x}, \\ F &= I_4 / \sqrt{-I_2\nu} = \psi / \sqrt{-U_\infty\nu x}, \\ E &= I_5 / \sqrt{-I_2^3\nu} = R / \sqrt{-U_\infty^3\nu/x} \end{aligned} \quad (13)$$

(negative I_2 due to $U_\infty < 0$ in Fig. 1). Substituting (13) and (11) into (4) we obtain

$$F_{\alpha\alpha\alpha} + (1+\beta)FF_{\alpha\alpha}/2 - \beta F_\alpha^2 + \beta + E_\alpha - \gamma F_{\alpha\alpha} = 0, \quad (14)$$

which describes a class of the self-preserving flows. Here, γ represents the dimensionless blowing and suction velocity. For $\beta = 0$ (ZPG), $E = 0$ (laminar flow), and $\gamma = 0$ (nonpenetrating wall), (4) is the Blasius equation for laminar boundary layers. For nonzero β with $E = \gamma = 0$, (4) is the Falkner-Skan family of boundary layers, with an exact analytical solution for $\beta = -1$ (i.e.,

$F_\alpha = 3 \tanh^2[\alpha + \tanh^{-1} \sqrt{2/3}] - 2$ [10]. Moreover, for $\beta = -1$ with nonzero E and γ , (4) becomes

$$F_{\alpha\alpha} + F_\alpha^2 - 1 + E_\alpha - \gamma F_{\alpha\alpha} = 0, \quad (15)$$

which is the self-preserving form of the sink-flow TBL with blowing and suction effects. Note that (15) has been obtained by [5] (for $\gamma = 0$) and [18] (for $\gamma \neq 0$) by dimensional analysis (assuming a specific self-similarity). However, the symmetry analysis here is more straightforward (the advantage as emphasized in [10]) resulting from the NSBL equation, and (14) is more general than (15) which indicates that there may exist other equilibrium flows with different values of β and γ (an open issue for future study).

Several interesting results can be deduced for $\beta = -1$. First, it is derived from the definition that the wall friction velocity $u_\tau \equiv \sqrt{-v\partial_y U|_{y=0}} = -U_\infty \sqrt{F_{\alpha\alpha}|_{\alpha=0} K_p}$ scales the same as the free-stream velocity, i.e., $u_\tau \propto -U_\infty$ (since $K_p = \sqrt{-vx^{-1}U_\infty^{-1}}$ is a constant). Then, the similarity variable α (dimensionless invariant) in (15) actually scales the same as the viscous unit, i.e., $\alpha = y^+ U_\infty^+ \sqrt{K_p} \propto y^+$, and (15) can be rewritten as

$$\frac{\partial^2 U^+}{\partial y^{+2}} + \frac{\partial R^+}{\partial y^+} = \gamma U_\infty^+ \sqrt{K_p} \frac{\partial U^+}{\partial y^+} - K_p U_\infty^+ (U_\infty^{+2} - U^{+2}), \quad (16)$$

where superscript $+$ denotes viscous normalization, i.e., $y^+ = yu_\tau/v$, $U_\infty^+ = -U_\infty/u_\tau$, $U^+ = -U/u_\tau$, $R^+ = R/u_\tau^2$, and $V^+ = V/u_\tau$ (all normalized variables are positive). A validation of (16) is shown in Fig. 2, in agreement with our theoretical descriptions obtained from (37)–(39) (explained later). Note that superficially (16) shows no explicit Re dependence, but in fact the latter is contained in the pressure gradient parameter K_p . In the DNS data of [18], $K_p \approx 7.71 \times 10^{-7}$ is fixed while the dimensionless blowing and suction strength $\gamma = V_w/\sqrt{-U_\infty v/x}$ (invariant along the stream) varies within a typical range from -0.34 to 0.68 . This thus allows us to focus on the wall blowing and suction effects here, leaving the K_p effect for future study (we hence omit the K_p dependence below).

Moreover, an exact relation between U^+ and V^+ following the definition (3) is obtained:

$$V^+ = V_w^+ - K_p U_\infty^+ y^+ U^+. \quad (17)$$

Here $\psi = vF/\sqrt{K_p}$ and $\psi_x/u_\tau = K_p U_\infty^+ y^+ U^+$ are substituted (note also $V_w^+ = V_w/u_\tau$). The comparison with DNS data [18] is shown in Fig. 2. Note that the remarkable linear slope extends from the wall to the entire flow region. The data agree with the theoretical $K_p U_\infty^+$ in (17) closely, thus validating the above analysis.

III. A SIMILARITY TRANSFORMATION FOR DIFFERENT γ 'S

We pursue the following question, i.e., how the wall blowing and suction influences the mean velocity. To address this, let us recall a similar problem in compressible flows where the mean velocity is altered by the density variation. Through the well-known van Driest transformation, different mean velocities at different M 's (Mach numbers) are transformed into a universal profile at $M = 0$ [19,20]. Similarly, it is natural to make an analogy that mean velocities at different γ 's would be transformed to be the universal one at $\gamma = 0$, when wall blowing and suction effects are considered in a proper way [see Figs. 3(a) and 3(b)]. This is formally expressed as

$$U_*^+(y^+, 0) = \int \phi S^+(y^+, \gamma) dy^+, \quad (18)$$

where U_*^+ is the mean velocity at $\gamma = 0$, i.e., $U_*^+ = U^+(y^+, 0)$; $\phi(y^+, \gamma)$ is the weighting function, and $S^+(y^+, \gamma) = \partial_{y^+} U^+$ is the mean shear obtained from mean velocity profile $U^+(y^+, \gamma)$ for blowing and suction conditions. Note that ϕ is a function of mean density in the van Driest transformation; here ϕ is unknown *a priori*, whose determination (as below) thus achieves a

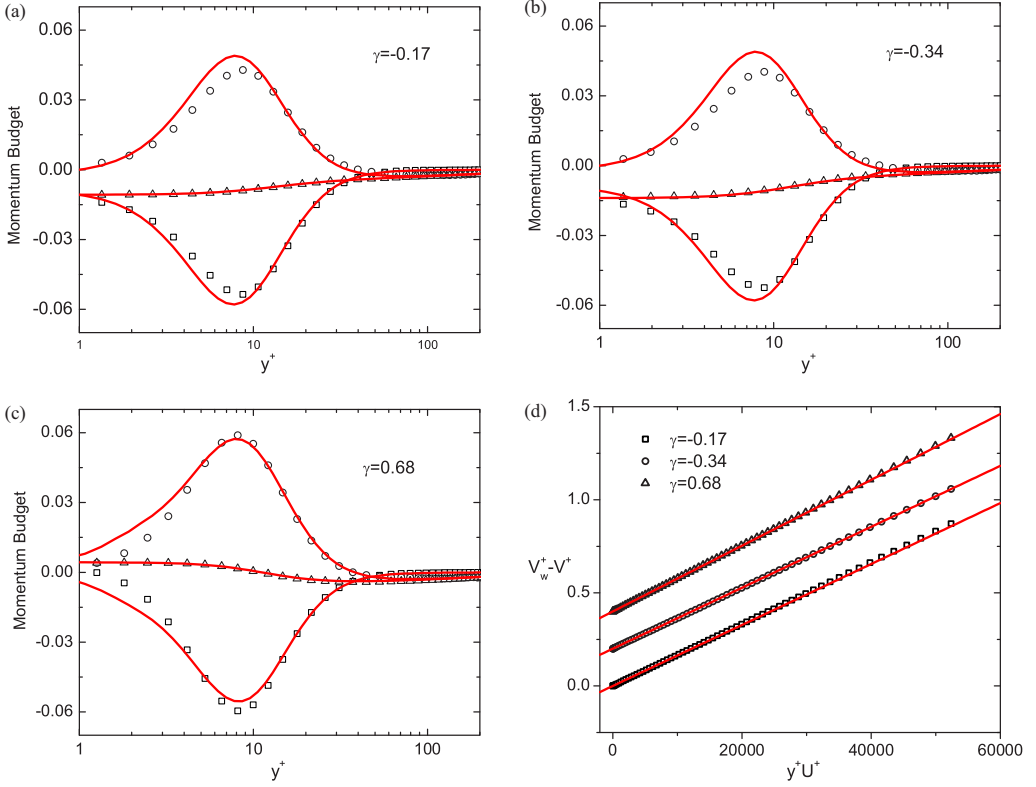


FIG. 2. (a)–(c) Budgets of (16); symbols, DNS data [18] for $\gamma = -0.17, -0.34$, and 0.68 ; lines, theoretical description; squares, $\partial^2 U^+ / \partial y^{+2}$; circles, $\partial R^+ / \partial y^+$; and triangles, the right-hand side of (16). (d) Verification of the linear relation between V^+ and U^+ for different γ 's where lines denote (17). Each profile has been vertically shifted by 0.2 for better display.

quantitative characterization of the blowing and suction effects. To emphasize, the existence of such a ϕ in (18) is nontrivial, because it requires that the wall blowing and suction not only preserve the streamwise equilibrium condition, but also lead to a new similarity among different γ 's never addressed before.

In fact, (18) has a transparent physical meaning. To see this, let us differentiate (18) with y^+ and obtain $\phi^{-1} = S^+ / S_*^+$. The latter indicates that ϕ^{-1} is the relative variation of the mean shear $S^+(y^+, \gamma)$ divided by $S_*^+ = S^+(y^+, 0)$ in the case of the nonpenetrating wall. This is very much like the case in the rough pipes [21,22], where the mean flux in rough pipes subtracted by the smooth wall flux (the so called Hamas function) is the right quantity to reveal the similarity induced by roughness elements. This also inspires us to seek the expression of the ϕ function.

Note that the transformation (18) implies a γ -independent quantity $\phi S^+ (= S_*^+)$. It motivates us to study the symmetry of (16), where group invariants independent of γ can be calculated from the first principle. To extend the symmetries of (16), we take the derivative of (16) with respect to y^+ to obtain the PDE system:

$$S^+ = \partial_{y^+} U^+,$$

$$\frac{\partial^2 S^+}{\partial y^{+2}} + \frac{\partial^2 R^+}{\partial y^{+2}} = \gamma U_\infty^+ \sqrt{K_p} \frac{\partial S^+}{\partial y^+} + 2K_p U_\infty^+ U^+ S^+. \quad (19)$$

Here, K_p (pressure gradient) is a constant; U_∞^+ depends on γ ; and U^+ , S^+ , and R^+ depend on γ and y^+ . Then, using MAPLE, the infinitesimals for the symmetry transformation of (19) are

SIMILARITY TRANSFORMATION FOR EQUILIBRIUM ...

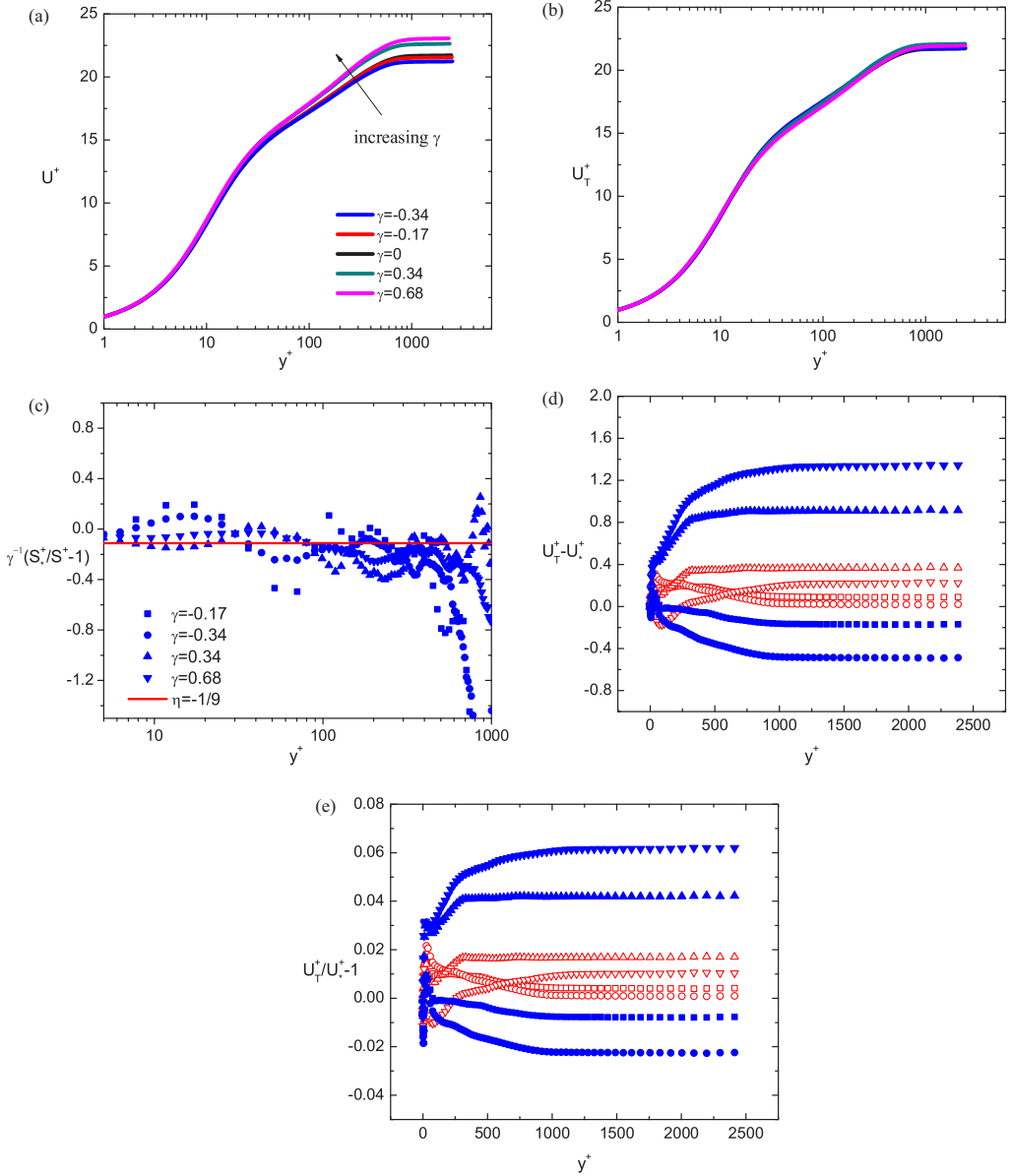


FIG. 3. A comparison of mean velocity profiles for different γ 's (a) before and (b) after transformations. (c) Measurement of $\eta = -1/9$ (line) by plotting $\gamma^{-1}(S_*^+/S^+ - 1)$ using DNS data. Note that scatters towards free stream are due to S_*^+ and S^+ approaching zero (hence S_*^+/S^+ is very sensitive to data). A comparison is shown of the departures before and after transformation, i.e., (d) $U^+ - U_*^+$ (solid symbols) versus $U_T^+ - U_*^+$ (open symbols) and (e) $U^+/U_*^+ - 1$ (solid symbols) versus $U_T^+/U_*^+ - 1$.

calculated:

$$\begin{aligned}\xi'_\gamma &= F_1, \\ \xi'_{y^+} &= (F_2/2)y^{+2} + F_3y^+ + F_4, \\ \eta'_{U^+} &= -\gamma F_2/(2\sqrt{K_p}) + (F_3 + F_5)U^+, \\ \eta'_{S^+} &= S^+(F_5 - F_2y^+),\end{aligned}$$

$$\begin{aligned}\eta'_{R^+} &= U^+ U_\infty^+ \sqrt{K_p} F_1 + (3S^+ / 2 + R^+ / 2 - \gamma U^+ U_\infty^+ \sqrt{K_p}) y^+ F_2 - 2\gamma U^+ U_\infty^+ \sqrt{K_p} F_3 \\ &\quad + (R^+ - \gamma U^+ U_\infty^+ \sqrt{K_p}) F_5 + (R^+ + S^+) F_6 + F_7 y^+ + F_8, \\ \eta'_{U_\infty^+} &= -(y^+ F_2 / 2 + 3F_3 + F_5 - F_6) U_\infty^+, \end{aligned} \quad (20)$$

where F_i ($i = 1, \dots, 8$) are arbitrary functions of γ and U_∞^+ . The corresponding characteristic equations for group invariants are

$$\frac{d\gamma}{F_1} = \frac{dS^+}{(F_5 - F_2 y^+) S^+} = \frac{dy^+}{(F_2 / 2) y^{+2} + F_3 y^+ + F_4} = \dots \quad (21)$$

Since our goal is a γ -independent ϕS^+ , we focus on the invariant composed only of γ and S^+ by integrating the first equation in (21), i.e.,

$$I_S = \ln(S^+) - \int (F_5 / F_1) d\gamma + y^+ \int (F_2 / F_1) d\gamma. \quad (22)$$

Therefore, I_S and any function of I_S are also group invariants independent of γ . While this gives a general expression for a γ -independent quantity, we need to further identify the explicit expression of ϕS^+ . As shown below, ϕS^+ is indeed a function of I_S and hence also a group invariant in most of the flow region (where $S^+ \ll 1$ or $S^+ \approx 1$). This is important because it supports that $S_*^+ = \phi S^+$ is indeed a γ -independent quantity based on the first principle [i.e., the symmetry of (19)].

Below we start to derive an analytical ϕ once the mean velocity profile $U^+(y^+, \gamma)$ is known. At first, integrating (16) from 0 to y^+ yields

$$S^+ + M^+ = 1, \quad (23)$$

where M^+ is the sum of the shear stress (RS), the pressure gradient effect (PG), and the mean vertical convection (VC), i.e.

$$M^+(y^+, \gamma) = \underbrace{R^+}_{\text{RS}} + \underbrace{K_p y^+ U_\infty^{+3}}_{\text{PG}} - \underbrace{\gamma \sqrt{K_p} U_\infty^+ U^+ - K_p U_\infty^+ \int_0^{y^+} U^{+2} dy'}_{\text{VC}}. \quad (24)$$

By dimensional analysis, a characteristic length function is introduced:

$$\ell^+(y^+, \gamma) = \sqrt{M^+ / S^+} = \sqrt{1 - S^+ / S^+}. \quad (25)$$

Therefore,

$$\frac{\ell^+}{\ell_*^+} = \frac{\sqrt{1 - S^+ / S^+}}{\sqrt{1 - S_*^+ / S_*^+}} = \frac{\phi \sqrt{1 - S^+}}{\sqrt{1 - \phi S^+}}, \quad (26)$$

where $\ell_*^+ = \ell^+(y^+, 0)$. Then, (26) leads to an important expression for ϕ in terms of S^+ and ℓ^+ / ℓ_*^+ , i.e.,

$$\phi = 2\xi / [1 + \sqrt{1 + 4\xi(\xi - 1) / (\ell^+ / \ell_*^+)^2}], \quad (27)$$

where $\xi = 1 / S^+$ ($= 1 / \partial_{y^+} U^+$). Now, the key is to estimate ℓ^+ / ℓ_*^+ as below. Considering that the moderate blowing and suction effect is indicated by a small parameter $|\gamma| < 1$ (validated by all the data here), an expansion of $\ell^+(y^+, \gamma)$ in γ is thus

$$\ell^+(y^+, \gamma) = \ell_*^+ (1 + \eta\gamma + \eta'\gamma^2 + \text{higher-order terms}), \quad (28)$$

where coefficients $\eta = \partial_\gamma(\ell^+ / \ell_*^+) |_{\gamma=0}$ and $\eta' = \frac{1}{2} \partial_\gamma[\partial_\gamma(\ell^+ / \ell_*^+)] |_{\gamma=0}$ are generally functions of y^+ . For simplicity, the expansions are truncated at the first order, i.e., $\ell^+ \approx \ell_*^+ (1 + \eta\gamma)$, which, after a substitution into (27), yields

$$\phi \approx 2\xi / [1 + \sqrt{1 + 4\xi(\xi - 1) / (1 + \eta\gamma)^2}] \quad (29)$$

and hence

$$S_*^+ = \phi S^+ \approx 2/[1 + \sqrt{1 + 4\xi(\xi - 1)/(1 + \eta\gamma)^2}]. \quad (30)$$

The relation between (30) and the symmetries of (19) is further discussed here. Note that for $\xi = 1/S^+ \gg 1$ or $S^+ \ll 1$ (data showing $S^+ < 0.1$ beyond the buffer layer edge $y^+ \approx 30$), (30) approximates to

$$S_*^+ = \phi S^+ \approx 2/[1 + \sqrt{1 + 4\xi^2/(1 + \eta\gamma)^2}]. \quad (31)$$

Importantly, ϕS^+ in (31) is indeed a function of the group invariant I_S , i.e.,

$$\begin{aligned} \phi S^+ &\approx 2/[1 + \sqrt{1 + 4\xi^2/(1 + \eta\gamma)^2}] \\ &= 2/[1 + \sqrt{1 + 4/(e^{I_S})^2}]. \end{aligned} \quad (32)$$

Here, after substituting the following specific conditions in (22), i.e.,

$$F_5 = -\eta F_1/(1 + \gamma\eta), \quad F_2 = 0, \quad (33)$$

the invariant I_S is given as

$$I_S = \ln(S^+) + \ln(1 + \gamma\eta). \quad (34)$$

Therefore, (32) tells us that ϕS^+ in (31) is also a group invariant and, hence, independent of γ and equal to S_*^+ . Note that Eqs. (20) and (33) are permitted by (19), but not by (16), due to the cubic term U_∞^{+3} in (16). Furthermore, the above analysis also applies to $\xi \approx S^+ \approx 1$ (viscous sublayer), where (30) approximates to $S_*^+ \approx S^+ \approx 1$. The latter is of course a group invariant with $F_5 = F_2 = 0$ in (20); this result trivially follows from the Taylor expansion $U_*^+ \approx U^+ \approx y^+$ at the wall.

The value of η is empirically measured as below. From (29), $\phi \approx 1 + \eta\gamma$ for $\xi \gg 1$, indicating $\eta \approx \gamma^{-1}(\phi - 1)$ for $y^+ \gg 1$. Therefore, we use DNS to evaluate η by plotting $\gamma^{-1}(S_*^+/S^+ - 1)$ [see Fig. 3(c)], which is suggested as

$$\eta \approx -1/9. \quad (35)$$

Note that values of η between -0.12 and -0.10 improve the collapse of the velocity profiles, and we therefore set it to $-1/9$, which is very close to -0.11 . Currently we do not have a clear physical explanation of $\eta = -1/9$, although it may have an interpretation in the future. In other words, η is currently derived empirically rather than theoretically. Also, there is larger data scatter towards the outer flow; this is because both S_*^+ and S^+ approach zero in the outer flow, hence their ratio is rather sensitive to the data quality. Here the negative sign indicates that ℓ^+ decreases with increasing γ , which is physical. This is because a larger γ indicates more mean vertical convection to be compensated by pressure force in (24), hence a relatively smaller M^+ and a smaller ℓ^+ . An interesting topic for future study is how η depends on K_p and Re .

Therefore, we obtain the final transformation by substituting (29) with (35) into (18). Figure 3(a) shows notable departures of U^+ profiles from each other before the transformation, and the departures increase apparently with increasing wall distance. In contrast, Fig. 3(b) shows the transformed velocities (U_T^+) according to (18), which remarkably collapse onto the universal one U_*^+ for the entire flow region. To display the quality of the collapse, Fig. 3(d) compares $U_T^+ - U_*^+$ (open symbols) with $U^+ - U_*^+$ (solid symbols). While the maximum difference between two velocity profiles before transformation is between $\gamma = -0.3417$ and $\gamma = 0.6834$, i.e., $\Delta U_{\max} = U^+(\infty, 0.6834) - U^+(\infty, -0.3417) \approx 1.8$, differences after transformation are mostly bounded within 0.4. We further plot $U_T^+/U_*^+ - 1$ in Fig. 3(e), which is bounded within 2% after the transformation. The collapse of data, although not an order of magnitude reduction, is still satisfactory since we only use a linear expansion for ℓ^+/ℓ_*^+ (i.e., a constant η).

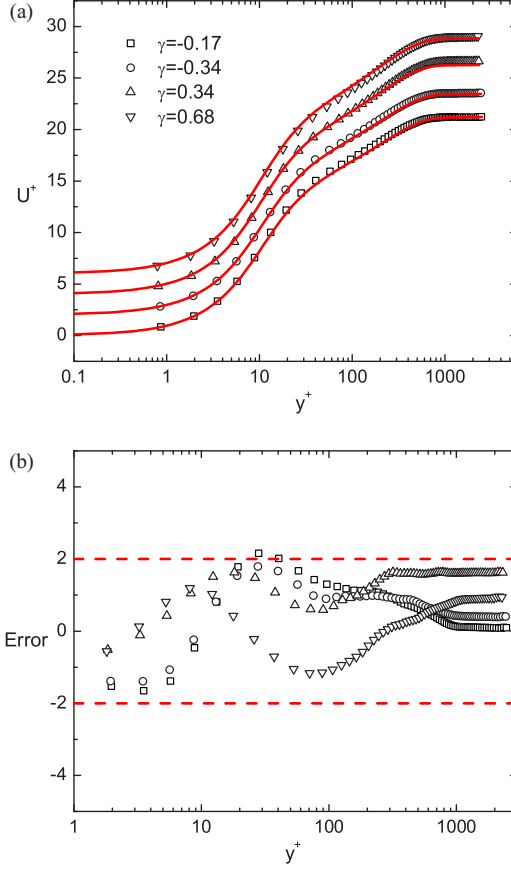


FIG. 4. Verification of (37). (a) Predicted \hat{U}^+ (lines) from U_*^+ by (37) compared with DNS data (symbols). Each profile has been vertically shifted (by 2) for better display. (b) Relative errors ($\times 100$) are uniformly bounded within 2% for the entire flow region.

The performance of the transformation (18) is further illustrated by a reverse transformation from U_*^+ to U^+ . In other words, we predict U^+ 's at different γ 's from the single profile $U_*^+(y^+)$. Note that, according to (27) and (29), we have

$$\begin{aligned} S^+ &= 2/[1 + \sqrt{1 + 4\xi^*(\xi^* - 1)(\ell^+/\ell_*^+)^2}] \\ &\approx 2/[1 + \sqrt{1 + 4\xi^*(\xi^* - 1)(1 + \eta\gamma)^2}], \end{aligned} \quad (36)$$

where $\xi^* = 1/S_*^+$ (and $\eta = -1/9$). Thus, by integrating (36) with y^+ , the resulting mean velocity is

$$\hat{U}^+ = \int S^+(\xi^*, \gamma) dy^+. \quad (37)$$

The results are shown in Fig. 4. One can see the agreement is very good and the relative errors are within 2% for the entire flow region. Note that one may introduce a damping function [23] to model ℓ^+ and hence obtain U^+ . This is another topic to be presented elsewhere.

Moreover, the wall normal mean velocity is given based on the single $U_*^+ y^+$ profile. According to (17) we have

$$\hat{V}^+ = \gamma \sqrt{K_p} \hat{U}_\infty^+ - K_p \hat{U}_\infty^+ y^+ \hat{U}^+, \quad (38)$$

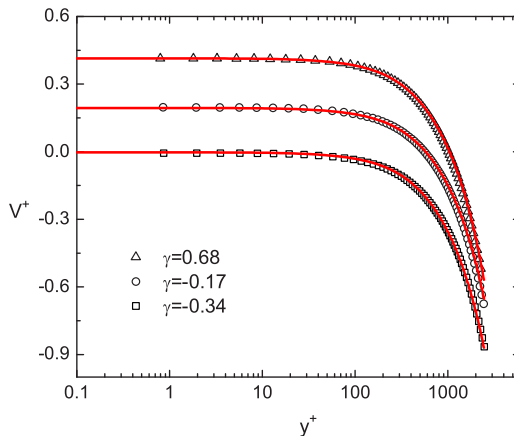


FIG. 5. Comparison of \hat{V}^+ from (38) with DNS data. Data are vertically shifted by 0.2 for each profile.

which indicates the wall normal velocity monotonically decreases from the wall due to the sink-flow constraint. Figure 5 shows the comparison between \hat{V}^+ and data, and the agreement is good. In addition, the Reynolds shear stress from (16) is

$$\hat{R}^+ = 1 - \partial_{y^+} \hat{U}^+ - \hat{U}_\infty^{+3} K_p y^+ + \gamma \sqrt{K_p} \hat{U}_\infty^+ \hat{U}^+ + K_p \hat{U}_\infty^+ \int_0^{y^+} \hat{U}^{+2} dy'. \quad (39)$$

Using (38) and (39), we thus calculate the budget of terms in (16), which is displayed in Figs. 2(a)–2(c), also in good agreement with data. The results in turn support well the similarity transformation (18).

IV. DISCUSSIONS AND CONCLUSIONS

We present a first similarity transformation for the mean velocities in sink-flow TBL with blowing and suction effects. It achieves a mapping of different U^+ 's at different blowing and suction strength γ 's into a universal U_*^+ at $\gamma = 0$. The result builds on a Lie group symmetry analysis which derives the self-similarity equation (ODE) for the mean mass and momentum, and unifies the Falkner-Skan equation and the sink-flow TBL with different pressure gradient and blowing and suction effects. Unlike dimensional analysis where there are various ways to combine primary variables, the dilation symmetry here straightforwardly leads to the similarity variables. The latter has been emphasized as an advantage of symmetry analysis by Cantwell [10], who has suggested it to be used along with dimensional analysis.

In the second part of this paper, a characteristic length is introduced whose first order expansion in γ leads to an analytical expression of the transformation. The latter is further shown to be a group invariant in the flow region where $S^+ \approx 1$ or $S^+ \ll 1$. Note that the expansion is key to the success of the transformation, which means that blowing and suction conditions can be effectively described by the relative variation (ratio) of length functions. Such a procedure (by characteristic lengths) was introduced by She *et al.* [22] as a new way to quantify turbulent wall flows (with more results to be presented). The accurate descriptions of the mean flow quantities from the single profile $U_*^+(y^+)$ indicate that the wall blowing and suction not only preserve the equilibrium condition but also lead to a new similarity among different γ 's.

A further discussion on the meaning of the dilation symmetry is presented here. Note that (9) means that if $U(x, y)$ is a solution of the sink-flow TBL, $U^* = e^{-\epsilon} U$, $x^* = e^\epsilon x$, $y^* = e^\epsilon y$ is also a solution. In other words, (9) implies a similarity solution of the form $U = x^{-1} f(y/x)$ for the sink-flow TBL, just like the Blasius similarity solution $U = g(y/\sqrt{x})$ for the flat plate laminar boundary

layer. As the former can be rewritten as $U^+ = f(y^+)$ since $u_\tau \propto x^{-1}$ and $y^+ = yu_\tau/\nu \propto y/x$, (9) also indicates that the mean velocity profiles at different streamwise locations would collapse when nondimensionalized by u_τ and y^+ . However, to emphasize, (9) does not result in any specific form of U^+ . The latter may allow the scaling such as the logarithmic law in the overlap region or the exponential law in the wake region as proposed by Oberlack [17]; nevertheless, these scalings are just “candidate” invariant solutions but not a direct consequence. This is the difference between our current work and that of Oberlack [17].

This work also opens several important issues which are explained briefly. The first is on the K_p effect. While the current study focuses on a specific K_p , more calculations are needed for different K_p 's to validate the transformation with an appropriate η . Second, towards a complete analytical description of mean velocity profiles [for instance, the $U_*^+(y^+)$], closure assumptions such as the mixing length model or the asymptotic logarithmic law can be introduced. Along this direction, a third-parameter paradigm, i.e., $\text{Re}_\theta - K_p - \gamma$, is expected in analogy to [4]. Third, it is important to delineate the γ range where the similarity transformation holds, as a huge intensive blowing and suction effect would break the similarity transformation and the equilibrium flow state. This is already mentioned in the preceding expansion analysis where $|\gamma| < 1$ is noted. Finally, a similar analysis can be carried out for the sink-flow TBL with different roughness effects [24]. Note that extending the current work to source flows would be interesting to determine if the rich variety of similarity flow states [25,26] would be broken by blowing and suction. All these to be pursued in the future are essential to the fundamental understanding of turbulent wall flows.

ACKNOWLEDGMENTS

This work benefited from discussions with Z. S. She of Peking University. We thank O. N. Ramesh for sharing the DNS data from his Ph.D. student S. S. Patwardhan [18].

APPENDIX: SYMMETRIES OF (4)

More symmetries of (4) can be calculated by using algebraic software. Below are the results obtained by using MAPLE:

$$\begin{aligned}
 \xi'_x &= G_1(x), \\
 \xi'_y &= (1 + \dot{G}_1/2)y + G_2(x, U_\infty, V_w), \\
 \eta'_\psi &= (\dot{G}_1/2 - 1)\psi + G_3(x), \\
 \eta'_R &= -(\dot{G}_1/2 + 3)R + \partial_x G_4(x, y) + G_5(x, U_\infty, V_w), \\
 \eta'_{U_\infty} &= -2U_\infty + \partial_y G'_4/U_\infty, \\
 \eta'_{V_w} &= -(\dot{G}_1/2 + 1)V_w + \psi \ddot{G}_1/2 + \dot{G}_3,
 \end{aligned} \tag{A1}$$

where ξ'_i and η'_i are infinitesimals for independent and dependent variables, respectively; the overdot indicates $\dot{G} = dG/dx$ and $\ddot{G} = d^2G/dx^2$. Note that (A1) is equivalent to the dilation group (9) by letting $G_2 = G_3 = G_4 = G_5 = 0$ and $G_1 = -2x/\beta$. Also note that due to the boundary condition ($U = R = \psi = 0$ at the wall) with the fixed sink apex, no translation or rotation is permitted. In this paper, we focus on the dilation group (9) in analogy to the Blasius equation for laminar flows, and the resulting symmetry is sketched in Fig. 1.

- [1] A. A. Townsend, *The Structure of Turbulent Shear Flow*, 2nd ed. (Cambridge University Press, Cambridge, UK, 1976).
- [2] T. B. Nickels, Equilibrium turbulent boundary layers with lateral streamline convergence or divergence, *J. Fluid Mech.* **623**, 273 (2010).
- [3] I. Marusic, B. J. McKeon, P. A. Monkewitz, H. M. Nagib, A. J. Smits, and K. R. Sreenivasan, Wall-bounded turbulent flows at high Reynolds numbers: Recent advances and key issues, *Phys. Fluids* **22**, 065103 (2010).
- [4] M. Jones, I. Marusic, and A. E. Perry, Evolution and structure of sink-flow turbulent boundary layers, *J. Fluid Mech.* **428**, 1 (2001).
- [5] S. Dixit and O. Ramesh, Pressure-gradient-dependent logarithmic laws in sink flow turbulent boundary layers, *J. Fluid Mech.* **615**, 445 (2008).
- [6] P. R. Spalart, Numerical study of sink-flow boundary layers, *J. Fluid Mech.* **172**, 307 (1986).
- [7] D. Coles, Remarks on the equilibrium turbulent boundary layer, *J. Aeronaut. Sci.* **24**, 495 (1957).
- [8] M. Jones and B. Launder, Some properties of sink-flow turbulent boundary layers, *J. Fluid Mech.* **56**, 337 (1972).
- [9] S. Dixit and O. Ramesh, Large-scale structures in turbulent and reverse-transitional sink flow boundary layers, *J. Fluid Mech.* **649**, 233 (2010).
- [10] B. J. Cantwell, *Introduction to Symmetry Analysis* (Cambridge University Press, Cambridge, UK, 2002).
- [11] A. Perry, I. Marusic, and J. Li, Wall turbulence closure based on classical similarity laws and the attached eddy hypothesis, *Phys. Fluids* **6**, 1024 (1994).
- [12] V. Patel and M. Head, Reversion of turbulent to laminar flow, *J. Fluid Mech.* **34**, 371 (1968).
- [13] A. A. Townsend, *The Structure of Turbulent Shear Flow*, 1st ed. (Cambridge University Press, Cambridge, UK, 1956).
- [14] J. C. Rotta, Turbulent boundary layers in incompressible flow, *Prog. Aeronaut. Sci.* **2**, 1 (1962).
- [15] N. K. Ibragimov, *CRC Handbook of Lie Group Analysis of Differential Equations* (CRC Press, Boca Raton, FL, 1994).
- [16] Z. S. She, X. Chen, and F. Hussain, Quantifying wall turbulence via a symmetry approach: A Lie group theory, [arXiv:1112.6312](https://arxiv.org/abs/1112.6312).
- [17] M. Oberlack, A unified approach for symmetries in plane parallel turbulent shear flows, *J. Fluid Mech.* **427**, 299 (2001).
- [18] S. Patwardhan, Effect of favourable pressure gradient on turbulence in boundary layers, Ph.D. thesis, Indian Institute of Science, Bangalore, 2014. <https://www.researchgate.net/profile/Saurabh-Patwardhan/publication>
- [19] E. Van Driest, Turbulent boundary layers in compressible fluids, *J. Aeronaut. Sci.* **18**, 145 (1951).
- [20] Y. S. Zhang, W. T. Bi, F. Hussain, X. L. Li, and Z. S. She, Mach-Number-Invariant Mean-Velocity Profile of Compressible Turbulent Boundary Layers, *Phys. Rev. Lett.* **109**, 054502 (2012).
- [21] J. Jiménez, Turbulent flows over rough walls, *Annu. Rev. Fluid Mech.* **36**, 173 (2004).
- [22] Z. S. She, Y. Wu, X. Chen, and F. Hussain, A multi-state description of roughness effects in turbulent pipe flow, *New J. Phys.* **14**, 093054 (2012).
- [23] S. B. Pope, *Turbulent Flows* (Cambridge University Press, Cambridge, UK, 2000).
- [24] J. Yuan and U. Piomelli, Numerical simulations of sink-flow boundary layers over rough surfaces, *Phys. Fluids* **26**, 015113 (2014).
- [25] H. K. Moffatt, Viscous and resistive eddies near a sharp corner, *J. Fluid Mech.* **18**, 1 (1964).
- [26] H. K. Moffatt and B. R. Duffy, Local similarity solutions and their limitations, *J. Fluid Mech.* **96**, 299 (1980).